Supporting information

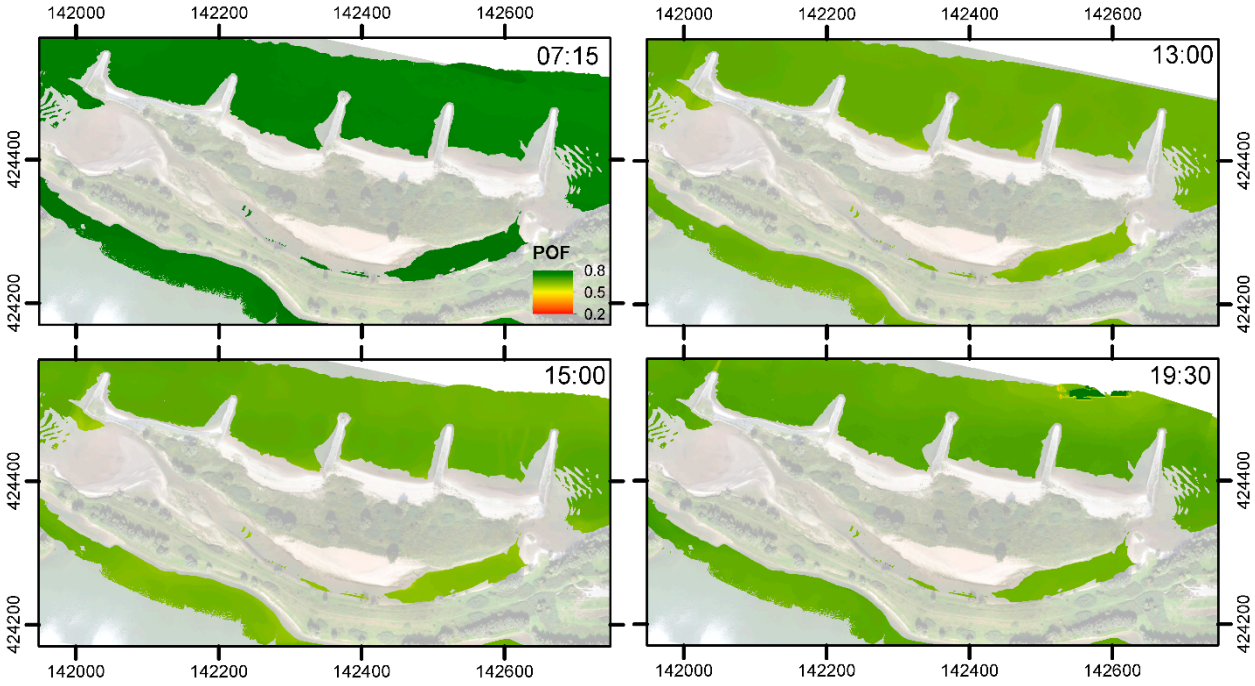

Fig. S1. The potentially occurring fraction (POF) of alien species in the river Waal near Gameren derived from remotely sensed water temperatures at 50 cm depth during a hot summer day.

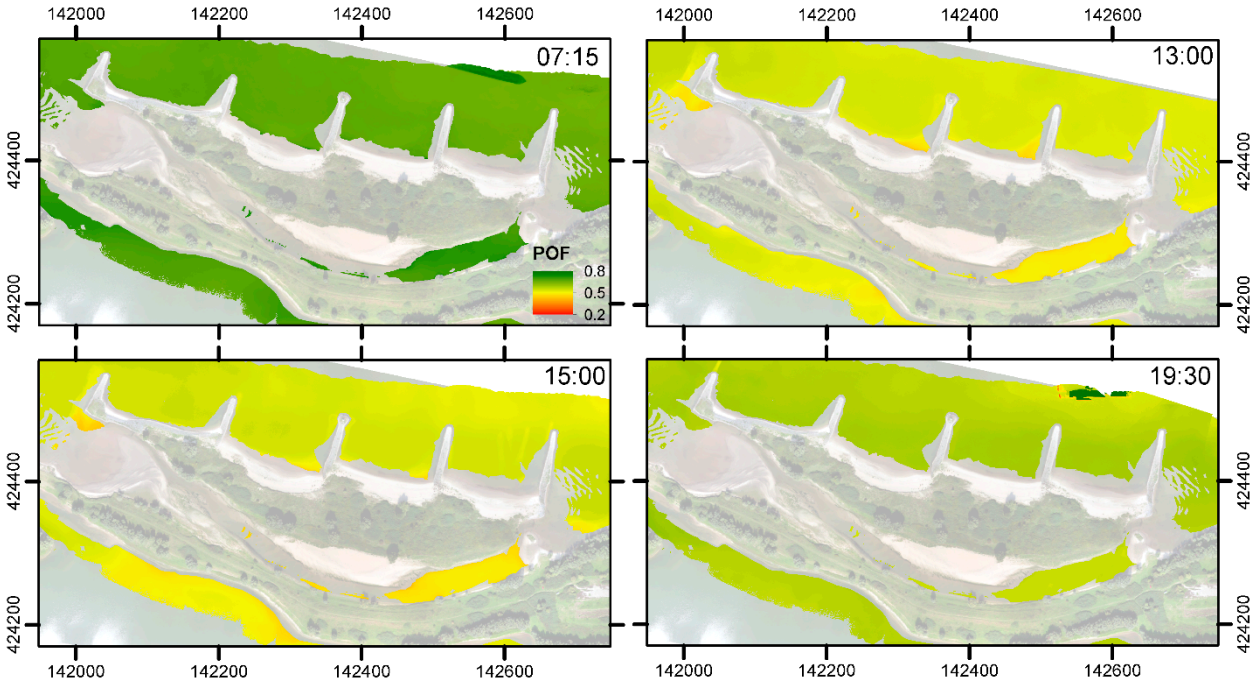

Fig. S2. The potentially occurring fraction (POF) of native species in the river Waal near Gameren derived from remotely sensed water temperatures at 50 cm depth during a hot summer day.

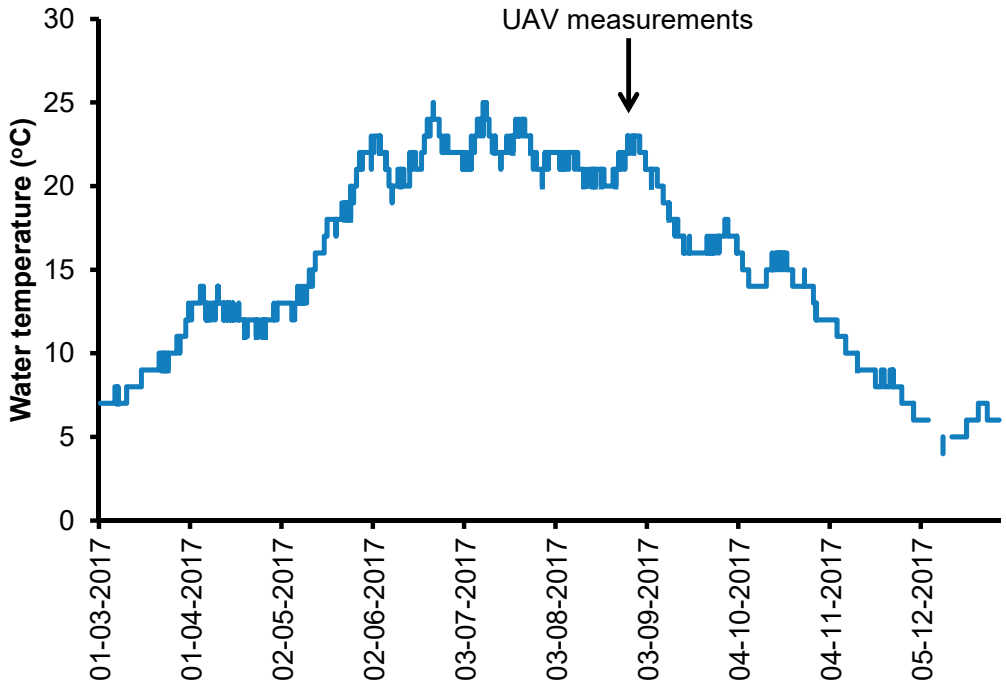

Fig. S3. Measured water temperatures in the river Rhine at gauging station Lobith during 2017.

Table S1 Literature overview of thermal remote sensing of surface water temperature.

Study object	Platform / Sensor	Resolution (m)	Wavelength (μm)	Validation method	Accuracy of RS measurement
Torgersen et al. 2001					
Oregon (USA), 50-60 km long sections, width: 2-110 m	Helicopter / Thermovision 1000 forward-looking infrared system (FLIR)	0.2 - 0.4	8 - 12	Onset thermometers at 10 cm depth (n=67)	MAE 0.3 °C y = 1.002 x - 0.018 (R^2 =0.99)
Handcock et al. 2006					
Green River, Yakima River, and Columbia River, USA, with stream widths between 10–500 m	Terra Satellite / MODIS Terra Satellite / ASTER Landsat-7 / Landsat ETM+ King Air B200 aircraft / MASTER Ground / FLIR	1000 90 60 5 and 15 0.05-0.5	6.54 - 14.39 8.12 - 11.65 10.40 - 12.50 10.15 - 11.45 10.15 - 11.45	Temperature loggers at stream bed (n =21) and portable thermometer at 10 cm depth	MD +1.2-2.2 °C for pure water pixels
Jensen et al. 2012					
Curtis Creek, Utah, 300 m long section of 5-10 m wide	AggieAir UAV / microbolometer thermal cameras by Infrared Cameras Inc.	0.30	*not reported*	Temperature samples (n=18)	Up to -7°C y = 0.7 x +8.2
Dugdale et al. 2015					
25 tributaries of the Restigouche River: 696 km total length, width unreported	Helicopter / FLIR SC660 uncooled microbolometer TIR camera	0.19	7 - 13	Onset HOBO UA-002-64 temperature loggers anchored to the river bed (n=32)	y = 0.95 x + 0.81 (R^2 =.97) RMSE = 0.45 °C
Fricke et al. 2015					
Two sections of the river Rhine of 237 km long and 150 to 500 m river wide	Aircraft / Image IR 8800 by InfraTec	4	8 - 12	Buoys with temperature loggers at 1 m depth (n=7)	MD −1.36 ± 0.16°C. y = 0.93 x -1.81
Fullerton et al. 2015					
Entire rivers varying from 50-645 km in USA	Aircraft / Different TIR sensors (similar wavelength range, radiometric calibration and sensitivity)	0.20 - 0.44	8 - 12	Instream Onset thermal sensors (n = not reported)	MAE 0.44 ± 0.37 °C
Iezzi et al. 2015					
Aterno River in Italy with 20 m width	Ground / FLIR Systems S65 HS portable thermal imager	*not reported*	7.5 - 13	Portable thermometer (n=9)	*not reported*
Wawrzyniak et al. 2016					
Ain River in France with a 60 m width	Aircraft / Thermo Tracer TH7800 and VarioCAM	0.6-1.5	8 - 14 7.5 - 14	VEMCO loggers at bottom of the river bed (n=7)	MAE 2.6±1.2 °C
This study					
Side channel river Waal, of 755 m long and max 40 m wide	Sensefly eBee / ThermoMAP	0.25	7-15	Onset thermometers at 10 (n=24) and 50 cm depth (n=4)	MAE 0.81 ± 0.60 y = 0.7469 x + 5.93 (R^2 =0.97) RSME 0.53 °C

* MAE = mean absolute error, MD = mean difference, RMSD = root mean squared difference

References Table S1

Dugdale, S. J., Bergeron, N. E., St-Hilaire, A., (2015) Spatial distribution of thermal refuges analysed in relation to riverscape hydromorphology using airborne thermal infrared imagery. Remote Sensing of Environment 160: 43-55.

Fricke, K., Baschek, B., (2015) Temperature monitoring along the Rhine River based on airborne thermal infrared remote sensing: estimation of in situ water temperatures and inflow detection compared to artificial satellite data. Journal of Applied Remote Sensing 9: 095067.

Fullerton, A.H., Torgersen, C.E., Lawler, J.J., Faux, R.N., Steel, E.A., Beechie, T.J., Leibowitz, S.G., (2015) Rethinking the longitudinal stream temperature paradigm: region-wide comparison of thermal infrared imagery reveals unexpected complexity of river temperatures. Hydrological Processes 29: 4719-4737.

Handcock, R.N., Torgersen, C.E., Cherkauer, K.A., Gillespie, A.R., Tockner, K., Faux, R.N., Tan, J., 2012. Thermal infrared remote sensing of water temperature in riverine landscapes, in: Fluvial remote sensing for science and management. John Wiley & Sons, New York, USA, pp. 85-113.

Iezzi, F., Todisco, M.T., (2015) Stream temperature estimated in situ from thermal-infrared images: best estimate and uncertainty. In Journal of Physics: Conference Series Vol. 655, No. 1, p. 012063. IOP Publishing, Italy.

Jensen, A.M., Neilson, B.T., McKee, M., Chen, Y., (2012) Thermal remote sensing with an autonomous unmanned aerial remote sensing platform for surface stream temperatures. In Proceedings IEEE Int. Geoscience and Remote Sensing Symposium (IGARSS), 2012, pp. 5049-5052.

Wawrzyniak, V., Piégay, H., Allemand, P., Vaudor, L., Goma, R., Grandjean, P., (2016) Effects of geomorphology and groundwater level on the spatio-temporal variability of riverine cold water patches assessed using thermal infrared (TIR) remote sensing. Remote Sensing of Environment 175: 337-348.

Torgersen, C.E., Faux, R.N., McIntosh, B.A., Poage, N.J., Norton, D.J., (2001) Airborne thermal remote sensing for water temperature assessment in rivers and streams. Remote Sensing of Environment 76: 386-398.